Desalination and Water Treatment
www.deswater.com

doi: 10.1080/19443994.2015.1129506

57 (2016) 22507–22518
October

Taylor & Francis
Taylor & Francis Group

Application of response surface methodology for the optimization of hexavalent chromium removal using a new low-cost adsorbent

Ezerie Henry Ezechi[a,*], Shamsul Rahman bin Mohamed Kutty[a], Mohamed Hasnain Isa[a], Mohd Shahir Liew[b]

[a]*Department of Civil and Environmental Engineering, Universiti Teknologi PETRONAS, Bandar Seri Iskandar, Perak 32160, Malaysia, Tel. +601 47395 339; email: honhenry2k5@yahoo.com (E.H. Ezechi), Tel. +605 368 7344; email: shamsulrahman@petronas.com.my (S.R.b.M. Kutty), Tel. +605 368 7346; email: hasnain_isa@petronas.com.my (M.H. Isa)*
[b]*Faculty of Geosciences and Petroleum Engineering, Universiti Teknologi PETRONAS, Bandar Seri Iskandar, Perak 32610, Malaysia, Tel. +605 368 7280; email: shahir_liew@petronas.com.my*

Received 23 December 2014; Accepted 3 December 2015

ABSTRACT

The adsorption capacity of a novel adsorbent (*Ageratum conyzoide* leaf powder) was investigated for Cr(VI) removal from aqueous solution. Experiments were designed with the Box–Behnken model of the response surface methodology (RSM). Preliminary experiments were conducted to obtain the optimum range of process variables used for the Box–Behnken model. Three independent variables (pH, initial concentration, and adsorbent mass) were examined. The results show that Cr(VI) removal was more favorable at pH 2. Increase in pH above 2 resulted in negative Cr(VI) removal. Cr(VI) removal increased when adsorbent mass was increased, but decreased with increase in initial concentration. Cr(VI) removal of 92% was obtained at pH 2 and adsorbent mass of 0.3 g. Experiments were successfully optimized by RSM. Kinetics study correlated with the pseudo-second-order kinetic model, whereas equilibrium study was best described by the Langmuir isotherm model with maximum adsorption capacity of 437 mg/g. Thermodynamic parameters indicate a spontaneous, exothermic, and physiosorption process.

Keywords: *Ageratum conyzoide* leaf powder; Adsorption; Box–Behnken; Chromium(VI); Equilibrium; Kinetic; Thermodynamic

1. Introduction

The presence of heavy metal ions in effluent wastewater can cause severe environmental and health problems. However, heavy metal ions such as chromium could commonly be present in effluent wastewater due to its wide industrial applications. Chromium has two major stable forms (hexavalent chromium and trivalent chromium), although other unstable valence states exist in biological systems [1]. Chromium have multifarious industrial applications such as in electroplating, leather tanning, textile dyeing, cement mining, dye manufacturing, aluminum conversion, coating operations, wood treatment, paints and pigments, photography industries, fertilizer production, and

*Corresponding author.

metal cleaning [2]. As a result, industrial effluents of high chromium concentration are discharged into the environment and aquatic systems [3].

Hexavalent chromium Cr(VI) is considered the most toxic form of chromium. In animals, it has a teratogenic effect and considered a potential carcinogen especially at low solubility. Occupational exposure to airborne chromium can result in irritative lesions of the skin and cancers of the respiratory tract [4]. In plants, chromium toxicity can result in reduced yield, inhibition of enzymatic activities, and mutagenesis [1]. The permissible limit for Cr(VI) discharge into inland surface waters is 0.1 and 0.05 mg/L in potable water [5]. Therefore, effective removal of Cr(VI) from industrial effluents is of paramount importance.

Contemporary treatment methods such as coagulation and flocculation, photocatalytic degradation, precipitation, solvent extraction, membrane processes, sonochemical techniques, biological processes, and integrated treatment processes have been used for Cr (VI) removal from wastewater [6]. However, some of their demerits are well documented [7]**.** Thus, suitable and cost-effective methods are required for Cr(VI) removal from industrial effluents.

Adsorption process has been widely used for the removal of various pollutants. Its comparative advantage over other treatment techniques include availability of adsorbent, ease of operation, and low cost. Commercial adsorbents such as activated alumina [8], silica gel [9], zeolite [10], and clays [11] were predominantly used due to their efficiency. However, the cost of commercial adsorbents hinders its maximum use. Thus, the shift toward nonconventional low-cost adsorbents derived from agricultural and solid waste sources such as groundnut husk [12], sawdust [13], rice husk ash [14], and olive bagasse [5] intensified.

Recently, adsorbents produced from agricultural plant leaves and roots have been widely utilized for adsorption process. Such adsorbents include water hyacinth plant [15], neem leaf powder [16], gulmohar plant leaf powder [17], and guava leaf powder [18]. Their advantages include less processing time, low cost, and high pollutant removal capacity [19].

Ageratum conyzoide is an annual plant of cultivated fields commonly found in tropical and subtropical regions. It invades farmlands and reduces the yield of major staple crops especially in rangeland areas. It suppresses native grasses and causes scarcity of fodder. It has high reproductive, competitive, and allelopathy potentials [20]. Nonetheless, *A. conyzoide* is widely used in traditional medicine for the treatment of various ailments. In the eastern part of Nigeria, its leaves are used as first aid for wound treatment. In India, the roots of *A. conyzoides* are useful against fever [21]. The essential oil of *A. conyzoides* inhibits afatoxin, a highly toxic and carcinogenic metabolite [22]. Its flowers and leaves have analgesic and anti-inflammatory properties [23]. However, investigation into its scientific application as adsorbent is still at infancy. Due to its abundance, it is considered a waste in most cases and unutilized.

Response surface methodology (RSM) is a statistical and mathematical technique used to develop, improve, and optimize processes. It could be used to evaluate the significance of several factors [24]. It proposes replicates at the center point to estimate error and predict model behavior based on results calculated at various points in the design space [25].

The optimum contact time and pH range for Cr (VI) have been determined [26]. The characterization of the adsorbent is reported elsewhere [19,27]. The objective of this study is therefore to optimize the adsorption of Cr(VI) from aqueous solution onto *A. conyzoides* using RSM, and determine the adsorption kinetics, isotherms, and thermodynamics.

2. Methodology

2.1. Adsorbent and adsorbate preparation

Fresh leaves of *A. conyzoides* were collected from the rural area of Tronoh, Perak, Malaysia as invasive plants. The leaves were severally washed with distilled water and dried for 48 h under sunlight. The dried leaves were rewashed with distilled water to remove surface impurities or dust and dried in an oven at 60˚C for 24 h. The leaves were then grounded with a domestic mixing grinder to yield fine particles of size 100–125 μm and were severally washed with distilled water to remove chlorophyll pigments. ACLP produced was then soaked in 5% HNO_3 to improve its porosity, redried at 60˚C for 24 h, and stored in a container for use. No further treatment was carried out on ACLP.

Stock solution (4,000 mg/L) of Cr(VI) was prepared by dissolving 11.31504 g of $K_2Cr_2O_7$ in 1 L deionized distilled water. Working concentrations were prepared by means of dilution. Batch adsorption experiments were conducted using 250-mL flask containing 100-mL Cr(VI) solution placed on an orbital shaker at 100 rpm. The ranges of process variables examined are pH (1–3), initial concentration (50–150 mg/L), adsorbent mass (0.1–0.3 g) at predetermined contact time (120 min). Initial solution pH was controlled using 0.1 M H_2SO_4 and NaOH, respectively. After each reaction time, the content of the flask was collected and filtered using 47 mm Whatman filter paper and analyzed for Cr(VI) residual concentration

using DR 2000 spectrophotometer (diphenycarbohydrazide method) at wavelength of 540 nm.

2.2. Adsorption study

Adsorption study was conducted using 100-mL solution containing various initial Cr(VI) concentrations. Adsorption time was varied and the amount of Cr(VI) adsorbed was calculated using the expression below:

$$q_e = (C_o - C_e)\frac{v}{w} \quad (1)$$

where C_o is initial Cr(VI) concentration (mg/L), C_e is equilibrium Cr(VI) concentration (mg/L), v is volume of sample (L), w is adsorbent mass (g).

The suitability of the kinetic models was evaluated using chi-square (χ^2) represented as [28]:

$$\chi^2 = \frac{(q_e^{(exp)}) - (q_e^{(cal)})^2}{(q_e^{(cal)})} \quad (2)$$

where $q_e^{(exp)}$ is the experimental adsorption capacity at equilibrium (mg/g), $q_e^{(cal)}$ is the calculated adsorption capacity at equilibrium (mg/g).

A low chi-square (χ^2) is desirable and indicates a low error component for the applicable model.

2.3. Equilibrium study

The equilibrium study was conducted using 100-mL solution containing different Cr(VI) concentrations. Adsorbent mass was varied at fixed contact time of 120 min.

2.4. Reaction dynamics

Thermodynamic parameters such as enthalpy (ΔH°) and entropy (ΔS°) were examined. A polyscience thermostatic warm water bath equipped with a corning stirrer was used to regulate reaction temperature and sample mixing. Thermodynamic constants were examined using the following equations [29]:

$$\Delta G^\circ = -RT \ln K_c \quad (3)$$

$$\ln K = \frac{\Delta S^\circ}{R} - \frac{\Delta H^\circ}{RT} \quad (4)$$

where K_c is distribution coefficient, R is thermodynamic gas constant (8.314 J/mol.K), T is temperature (k).

2.5. Adsorbent analysis

The microstructural properties of the adsorbent were characterized using scanning electron microscope (SEM, Zeiss Supra55 VP). The functional groups on ACLP were examined using Fourier transform infrared spectroscopy (FTIR) 4100. Adsorbent porosity, chemical composition, morphological characteristics, and isoelectric point are reported elsewhere [19].

3. Results and discussion

3.1. Adsorbent morphology

The ACLP micrographs obtained before and after adsorption are shown in Fig. 1a and 1b, respectively. ACLP consists of large pores on its surface before Cr (VI) adsorption as shown in Fig. 1a. However, these pores were reduced or filled after Cr(VI) adsorption as shown in Fig. 1b. The surface morphology of ACLP significantly contributed to the adsorption of Cr(VI).

The functional groups in FTIR spectroscopy of raw ACLP include C–H wag (–CH_2X) alkyl halides, N–H bend amines, C–H stretch alkanes, OH stretch H-bonded phenols and alcohols as shown in Fig. 2. The shift in the position of the functional groups of Cr(VI)-loaded ACLP in Fig. 2 could be attributed to the adsorption process.

3.2. Statistical design of experiment

Box–Behnken model of the RSM was used for model design. The independent process variables used were: pH (A), initial concentration (B), and adsorbent mass (C) across three levels as shown in Table 1. A total of 17 experiments was conducted with 5

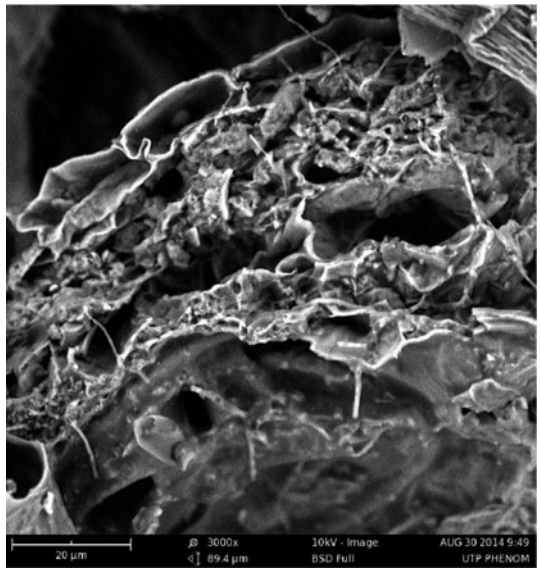

Fig. 1a. SEM micrograph of ACLP before use.

Fig. 1b. SEM micrograph of Cr(VI)-loaded ACLP.

replicates at the center for estimation of error. All results were triplicates of experimental runs.

The experimental data obtained from the model could be fitted to the second-order polynomial model in Eq. (5):

$$Y = \beta_0 + \sum_{j=1}^{k} \beta_j X_j + \sum_{j=1}^{k} \beta_{jj} X_j^2 + \sum_{i} \sum_{<j=2} \beta_{jj} X_i X_j + e_i \tag{5}$$

where Y is the response, X_i and X_j are variables, β_0 is a constant coefficient, β_j, β_{jj}, and β_{ij} are interaction coefficients of linear, quadratic, and the second-order terms, respectively, k is the number of studied factors, and e_i is the error.

The coded values of the process parameters in Eq. (5) could be determined by Eq. (6):

$$X_i = \frac{X_i - X_0}{\Delta X_i} \tag{6}$$

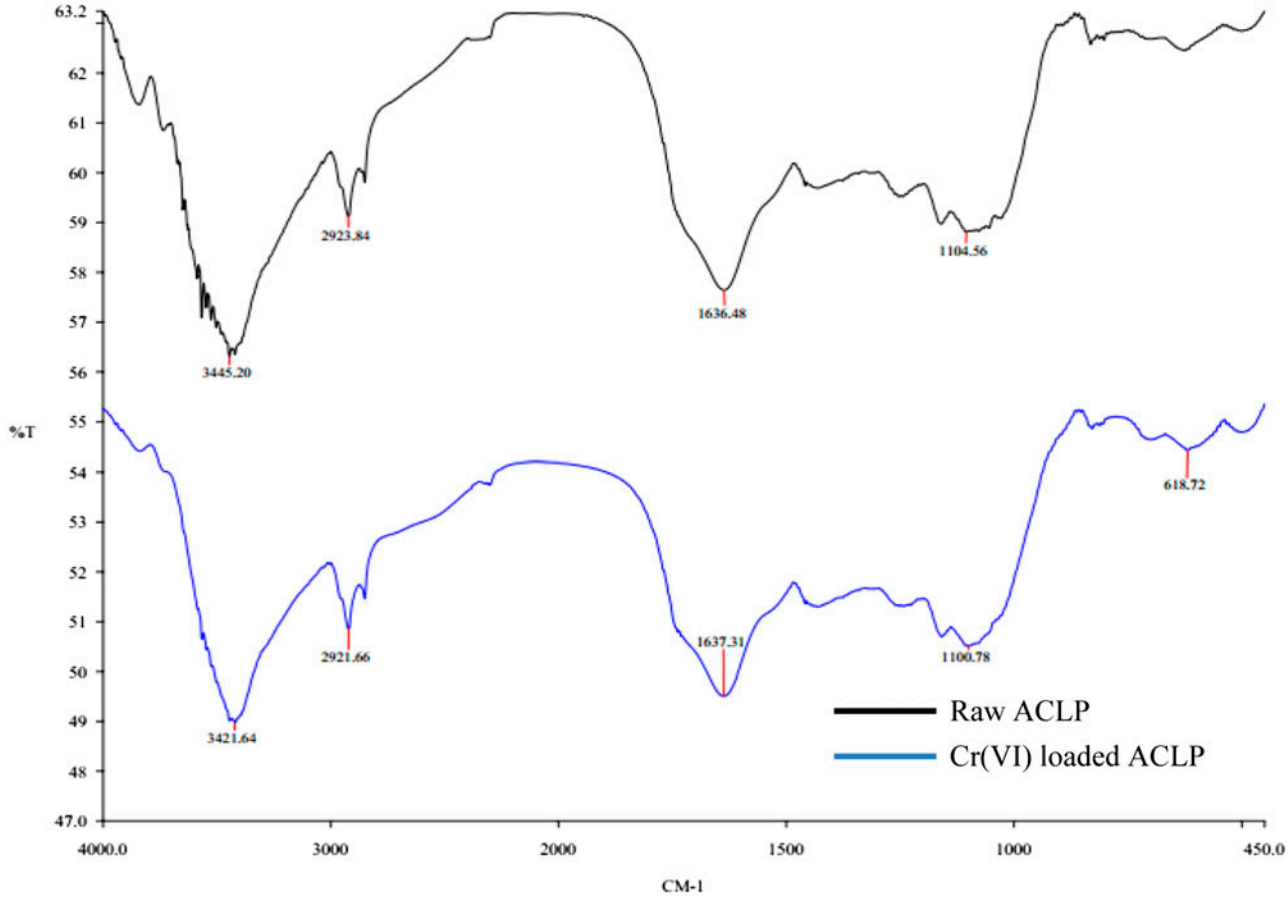

Fig. 2. FTIR Spectra of ACLP and Cr(VI)-loaded ACLP.

Table 1
Independent variables of the Box–Behnken design

Level of value	pH (*A*)	Concentration (mg/L) (*B*)	Adsorbent mass (g) (*C*)
−1	1	50	0.1
0	2	100	0.2
+1	3	150	0.3

where X_i is the uncoded value of the *i*th independent variable, X_0 is the uncoded *i*th independent variable at the center point, and ΔX_i is the step change value between low level (–1) and high level (+1).

The interactive effects between the independent variables and responses were analyzed by ANOVA. Statistical significance was examined by the *F*-test and correlation coefficient (R^2). Model terms were evaluated by the *p*-value (probability) with 95% confidence level. Three-dimensional plots were obtained for Cr (VI) removal. The experimental plan and the responses are presented in Table 2.

3.3. Analysis of variance

The analysis of variance (ANOVA) for the predicted response surface quadratic model was examined by Design Expert Software (8.0) and presented in Table 3 after exclusion of non-significant model terms. The model *F*-value of 111.62 and a low probability value (Prob. > F < 0.0001) confirm that the model is significant. Values of Prob. > F less than 0.0500 indicate that model terms are significant. Adequate precision evaluates the range of the predicted values at the design points and a value greater than 4 is desirable for a good model [30]. The adequate precision obtained in this study was 34.050. The correlation coefficient (R^2) of 0.9931 represents a sufficient signal for the model. The lack of fit test compares residual and pure errors at replicated design point. A significant lack of fit is undesirable and implies that the hypothesized model consist of unaccounted systematic variations [31]. The lack of fit in this study is not significant. Significant model terms in this study are *A* (pH), *B* (initial conc.), *C* (adsorbent mass), A^2 $(pH)^2$, B^2 (initial conc.)^2, C^2 (adsorbent mass)^2, *AB* (pH × initial conc.), and *AC* (pH × adsorbent mass). Based on the ANOVA analysis, the RSM model in this study was considered adequate. Table 3 indicates that pH has a more interactive effect than other variables. The probability *F*-values were higher for the interaction term *BC* (initial conc. × adsorbent mass). Thus, the final regression equation after the exclusion of *BC* (initial conc. × adsorbent mass) is expressed by the following second-order polynomial equation:

Table 2
Response and predicted values for different experimental conditions

S/N	*A*: pH	*B*: Cr(VI) conc. (mg/L)	*C*: Adsorbent dosage (g)	Response Cr(VI) (%)	Predicted values
1	1.00	50.00	0.20	42	43.98
2	3.00	150.00	0.20	56	75.40
3	3.00	100.00	0.10	69	35.47
4	1.00	100.00	0.30	59	54.02
5	3.00	100.00	0.30	72	33.12
6	2.00	100.00	0.20	81	69.31
7	2.00	100.00	0.20	78.7	58.69
8	1.00	150.00	0.20	36.6	72.47
9	2.00	100.00	0.20	81.3	77.49
10	2.00	50.00	0.10	79	61.01
11	3.00	50.00	0.20	74.2	90.32
12	1.00	100.00	0.10	33.6	76.91
13	2.00	50.00	0.30	92	81.36
14	2.00	100.00	0.20	83.1	81.36
15	2.00	100.00	0.20	82.7	81.36
16	2.00	150.00	0.30	75.4	81.36
17	2.00	150.00	0.10	59.3	81.36

Table 3
ANOVA result for response surface quadratic model and significant model terms

		Sum of squares	DF	Mean square	*F*-value	Prob. > *F*	
Model		4,819.29	9	535.48	111.62	<0.0001	Significant
	A	*1,248.33*	1	*1,248.33*	*260.21*	*<0.0001*	Significant
	B	*447.00*	1	*447.00*	*93.18*	*<0.0001*	Significant
	C	*412.80*	1	*412.80*	*86.05*	*<0.0001*	Significant
	A^2	*2,342.78*	1	*2,342.78*	*488.34*	*<0.0001*	Significant
	B^2	*129.93*	1	*129.93*	*27.08*	*0.0012*	Significant
	C^2	*166*	1	*166*	*35*	*0.0006*	Significant
	AB	*41.39*	1	*41.39*	*8.63*	*0.0218*	Significant
	AC	*125.44*	1	*125.44*	*26.15*	*0.0014*	Significant
	BC	*2.35*	1	*2.35*	*0.49*	*0.5065*	
	Residual	33.58	7	4.80			
	Lack of Fit	*21.55*	3	*7.18*	2.39	0.2097	Not significant

Notes: Std Dev. 2.19; R^2 = 0.9931; R^2 adj. = 0.9842; Pred. R^2 = 0.9251; Adeq. Prec. = 34.050; Press = 363.60.

$$\begin{aligned}\text{Cr(VI) removal}\,(\%) = {} & +81.36 + 12.49\,(\text{pH}) \\ & + 7.47\,(\text{initial conc.}) \\ & + 7.18\,(\text{mass of adsorbent}) \\ & - 23.59\,(\text{pH})^2 \\ & - 5.56\,(\text{initial conc.})^2 \\ & - 6.63\,(\text{mass of adsorbent})^2 \\ & - 3.32\,(\text{pH})\,(\text{inital conc.}) \\ & - 5.60\,(\text{pH})\,(\text{mass of adsorbent})\end{aligned} \tag{7}$$

The adequacy of the model was evaluated by the diagnostic plots in Fig. 3(a) and (b). The normal probability plot was approximately linear, whereas the predicted vs. actual value plot was close to each other. Thus, the diagnostic plots are in good agreement with the model.

3.4. Hexavalent chromium Cr(VI) removal

Three process variables were investigated for Cr(VI) adsorption onto ACLP. Two process variables were varied, whereas one parameter was fixed. Fig. 4a represents the plot of pH vs. initial concentration at fixed adsorbent mass of 0.2 g. pH was varied in the range 1–3 to ascertain the optimum point at close range. pH has a significant effect on Cr(VI) adsorption. Results show that when pH was raised from 1 to 2, Cr(VI) adsorption increased but decreased at pH 3. Cr(VI) adsorption was more favorable at pH 2 with removal of 92%. The effect of pH on Cr(VI) removal could be explained from the isoelectric point of ACLP. The isoelectric point of ACLP is 5.1 [19]. The adsorbent is positively charged below 5.1 and negatively charged above 5.1. It is well known that different species of Cr(VI) found in aqueous solution are highly pH dependent. According to the logarithmic concentration diagram of chromium, HCrO is the dominant form of Cr(VI) at low pH, whereas other forms of Cr(VI) such as CrO_4^{2-} and CrO_7^{2-} are dominant at higher pH (>5) [32–34].

Therefore, the effective removal of Cr(VI) at low pH values could be attributed to the dissociation of the functional groups (OH and CH) on the surface of ACLP active sites. At acidic pH, the functional groups protonates, attracting more Cr(VI) molecules. However, high Cr(VI) removal at pH 2 could be attributed to strong chemical interaction and electrostatic attraction with equal preference for molecular Cr(VI) ions (HCrO) between the charged adsorbent surface and the adsorbate. This observation is in agreement with other authors [35,36].

The effect of adsorbent mass is presented in Fig. 4a. Adsorbent mass was varied in the range 0.1–0.3 g. Cr(VI) adsorption increased with increase in adsorbent mass. Cr(VI) adsorption increased from 59.3 to 75.4% when adsorbent mass was raised from 0.1 to 0.3 g at pH 2 and initial Cr(VI) concentration of 150 mg/L. This could be due to the availability of more active sites at higher adsorbent mass. Similar observation is reported in the literature [13].

Cr(VI) adsorption decreased with increasing initial Cr(VI) concentration. Initial Cr(VI) concentration was varied in the range 50–150 mg/L. At all initial Cr(VI) elevation, residual Cr(VI) increased. Cr(VI) adsorption decreased from 74.2 to 56% when initial concentration was raised from 50 to 150 mg/L at pH 3 and adsorbent mass of 0.2 g. This could be attributed to insuffi-

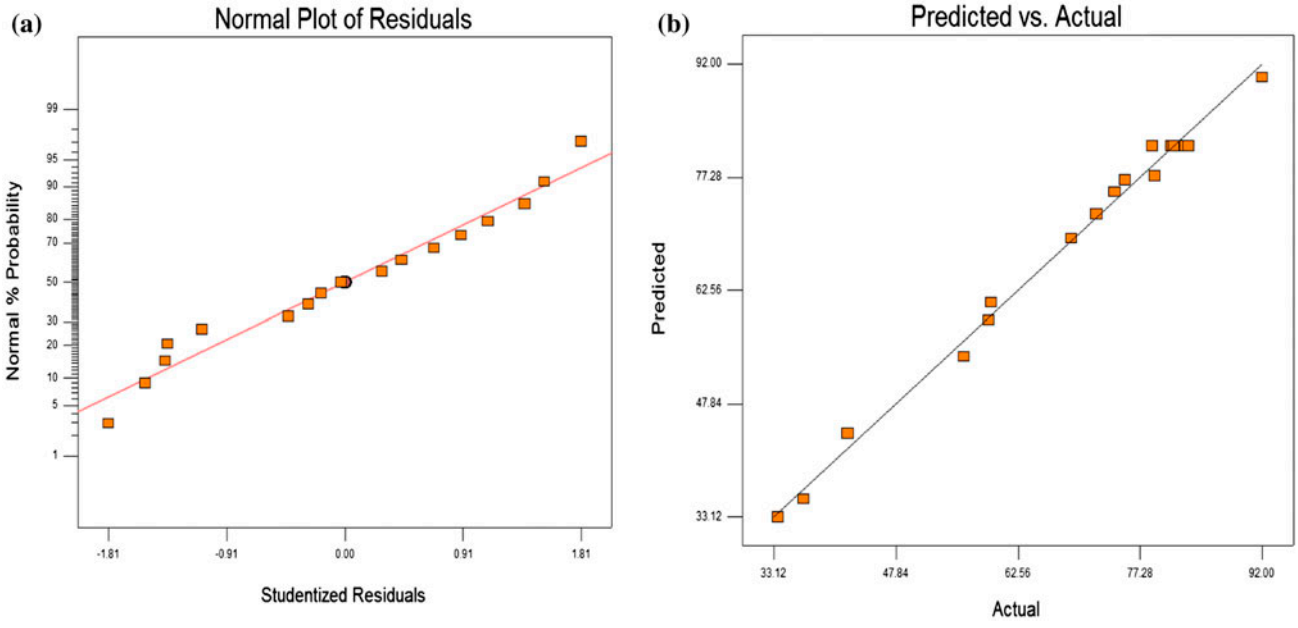

Fig. 3. (a) and (b) Diagnostics plots.

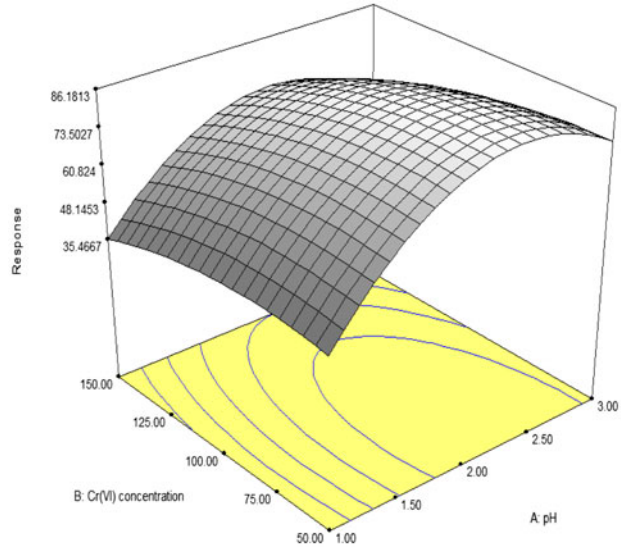

Fig. 4a. Contact time 120 min; volume of sample 100 mL (a) effect of pH and Cr(VI).

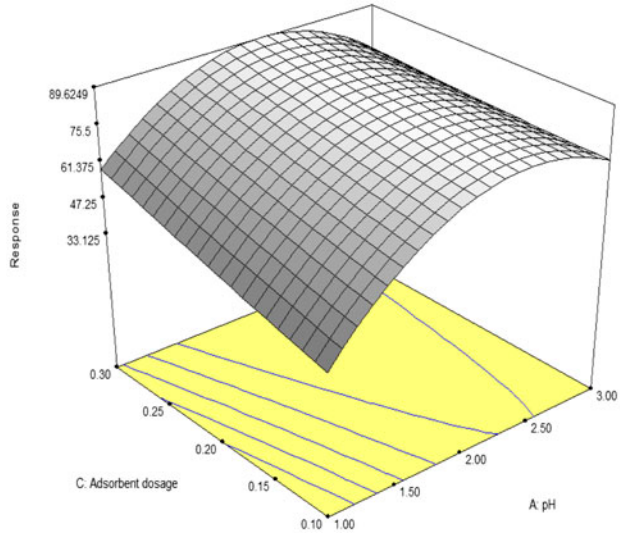

Fig. 4b. Effect of concentration.

cient active sites on the surface of ACLP at higher concentration. This is consistent with the report of other authors [13].

3.5. Process optimization

Numerical conditions for optimization of Cr(VI) adsorption onto ACLP were conducted using RSM. The goal for each process variable (pH, initial concentration, and adsorbent mass) was selected within range whereas the response Cr(VI) was defined as maximum to achieve the highest optimum performance. The model in Table 4 predicts a Cr(VI) removal of 91.03% from initial concentration of 66.51 mg/L. Experiments conducted under these conditions yielded a Cr(VI) removal of 91.9%. This confirms that the model was successfully optimized.

4. Adsorption kinetics

Adsorption kinetics were evaluated by the pseudo-first-order kinetic model, pseudo-second-order kinetic model, intraparticle diffusion, and Elovich model, respectively. The linearized forms of these models are represented below [37–40]:

$$\text{First order model} = \log(q_e - q_t) = \log(q_e) - \frac{k_1 t}{2.303} \quad (8)$$

$$\text{Second order model} = \frac{t}{q_t} = \frac{1}{k_2 q_e^2} + \frac{t}{q_e} \quad (9)$$

$$\text{Intraparticle diffusion} = q_t = K_{id} t^{0.5} + C_i \quad (10)$$

$$\text{Elovich model} = q_t = \frac{1}{\beta}\ln(\alpha\beta) + \frac{1}{\beta}\ln t \quad (11)$$

where q_e is amount adsorbed at equilibrium (mg/g), q_t is amount adsorbed at any time (t) (mg/g), k_1 (min) is the calculated pseudo-first-order rate constant, k_2 is the calculated pseudo-second-order rate constant (g/mg min), K_{id} (mg/g $\text{min}^{0.5}$) is a measure of the diffusion coefficient, C_i is the intraparticle diffusion constant (mg/g), α is the initial adsorption rate (mg/g.min), and β is the surface coverage (g/mg) during any experiment.

4.1. Pseudo-first-order kinetics

Kinetic constants for the pseudo-first-order model are presented in Table 5. Adsorption capacity (q_e) and rate constants (k_1) were calculated from the intercept and slope of the plot of $\log(q_e - q_t)$ vs. (t). The obtained correlation coefficient (R^2) was high (>0.870) for all concentration examined. However, the experimental adsorption capacity (q_e^{exp}) was not in agreement with the calculated adsorption capacity (q_e^{cal}). The chi-square (χ^2) was found to be high. This suggests that the pseudo-first-order kinetic model did not significantly describe adsorption of Cr(VI) onto ACLP.

4.1.1. Pseudo-second-order kinetics

The kinetic plot of t/q_t vs. t for the pseudo-second-order kinetic model is presented in Fig. 5. Adsorption capacity (q_e) and rate constants (k_1) were calculated from the slope and intercept. The kinetics constants in Table 5 shows a high correlation coefficient (R^2) (>0.992) for all concentration examined. The experimental adsorption capacity (q_e^{exp}) was in agreement with the calculated adsorption capacity (q_e^{cal}). The chi-square (χ^2) for all Cr(VI) concentration was low (<0.048). This suggests that the pseudo-second-order kinetic model suitably described Cr(VI) adsorption onto ACLP.

The initial rate of adsorption for the pseudo-second-order kinetic model is expressed as:

$$h = k_2 q_e^2 \quad (12)$$

where h is the initial adsorption rate (mol g^{-1} min^{-1}), k_2 is the pseudo-second-order rate constant (g mol^{-1} - min^{-1}), and q_e is the equilibrium adsorption capacity (mg/g).

The initial adsorption rate (h) increased with increasing initial Cr(VI) concentration (Table 5). Such increase could be attributed to the driving force of mass transfer from solutions of higher Cr(VI) to the vacant active pores of ACLP [19]. Maximum initial adsorption rate (h) of 40.49 mol g^{-1} min^{-1} was obtained at Cr(VI) concentration of 150 mg/L.

4.1.2. Intraparticle diffusion

The kinetic constants for the intraparticle diffusion plot of q_t vs. $t^{0.5}$ are presented in Table 5. The diffusion coefficient (K_{id}) and intraparticle rate constants (C_i) were determined from the slope and intercept, respectively. A high correlation coefficient (R^2) was obtained for all Cr(VI) concentration examined. The diffusion coefficient (K_{id}) and rate constant (C_i) increased with increasing Cr(VI) concentration. However, a deviation of the plot from the origin suggests that more than one transport mechanism was involved in the transfer of the analyte onto the solid surface.

Table 4
Numerical optimization

Solution no.	pH	Concentration (mg/L)	Adsorbent dose (g)	Cr(VI) (%)	Desirability
1	2.18	66.51	0.30	91.03	1.000

Table 5
Kinetic constants

Parameter values: Cr(VI) concentration (mg/L)				
Models	Parameters	50	100	150
First-order model: $\log(q_e - q_t) = \log(q_e) - (k_1 t/2.303)$	K_1	0.328	0.422	0.533
	$q_e^{(cal)}$	10.336	22.711	34.27
	R^2	0.99	0.871	0.978
	X^2	14.32	18.36	20.77
Second-order model: $t/q_t = 1/K_2 q_e^2 + t/q_e$	$K_2 \times 10^2$	0.0358	0.0113	0.0109
	$q_e^{(cal)}$	21.5	42.7	60.1
	R^2	0.997	0.993	0.994
	H	18.12	21.02	40.49
	X^2	0.047	0.004	0.012
Intraparticle diffusion: $q_t = K_{id} t^{0.5} + C_i$	K_i	11.77	27.75	43.68
	C_i	2.227	7.472	13.098
	R^2	0.978	0.979	0.978
Elovich model: $q_t = \frac{1}{\beta}\ln(\alpha\beta) + \frac{1}{\beta}\ln t$	α	6.225	15.114	23.111
	β	10.95	34.46	62.1
	R^2	0.933	0.992	0.934
Experimental data	$q_e^{(exp)}$	22.5	43.13	60.95

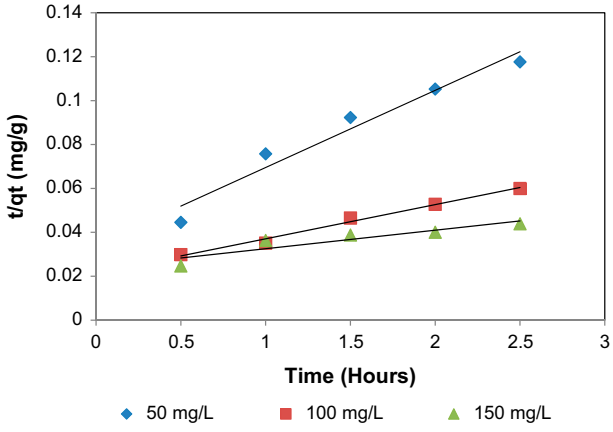

Fig. 5. Pseudo-second-order kinetics.

4.1.3. Elovich model

The Elovich rate equation is helpful in explaining predominantly, chemical adsorption on highly heterogenous adsorbents at initial stage [41]. The adsorption rate (α) and the surface coverage (b) in Table 5 were determined from the slope and intercept of the plot of q_t vs. ln t. The adsorption rate (α) and the surface coverage (b) increased with increasing Cr (VI) concentration. The correlation coefficient (R^2) was high. However, the pseudo-second-order kinetic have higher correlation coefficient (R^2).

Table 6
Langmuir and Freundlich isotherm constants

Langmuir constants		Freundlich constants	
q_{max} (mg/g)	437	K_f	0.0018
b	0.1	n	1.6
R^2	0.988	R^2	0.981
R_L	0.042	–	–

4.2. Equilibrium study

Equilibrium study was investigated using the Langmuir and Freundlich isotherms. The linearized

Table 7
Comparison of adsorption capacity of Cr(VI) on various adsorbents

Adsorbents	q_{max} (mg/g)	R^2	Refs.
Clarified sludge	26.31	0.9972	[14]
Rice husk ash	25.64	0.9901	[14]
Activated alumina	25.57	0.9916	[14]
Fuller's earth	23.58	0.9925	[14]
Fly ash	23.86	0.9917	[14]
Saw dust	20.70	0.9967	[14]
Neem bark	19.60	0.9966	[14]
ACLP	437	0.988	Present study

Table 8
Thermodynamic constants

Temp (K)	K_c	$(\Delta G)^\circ$ (kJ/mol)	$(\Delta H)^\circ$ (kJ/mol)	$(\Delta S)^\circ$ (J/mol.K)
297	2.4242	−2.1866		
307	1.3440	−1.2752	−23.41	−71.8
317	1.0238	−0.5890		
328	0.7850	−0.0386		

forms of these isotherm models are expressed below [42,43]:

$$\text{Langmuir isotherm} = \frac{C_e}{q_e} = \frac{1}{q_m b} + \frac{C_e}{q_m} \quad (13)$$

$$\text{Freundlich isotherm} = \log q_e = \log K_f + \frac{1}{n} \log C_e \quad (14)$$

where q_e is amount adsorbed at equilibrium concentration C_e, q_m is the Langmuir constant representing maximum monolayer adsorption capacity and b is the Langmuir constant related to energy of adsorption, K_f and n are constants affecting the adsorption capacity and intensity of adsorption, respectively.

The Langmuir isotherm constants for the plot of $1/q_e$ vs. $1/C_e$ are shown in Table 6. Maximum adsorption capacity (q_{max}) and the energy of adsorption (b) were determined from the slope and intercept, respectively. A high correlation coefficient (R^2) value of 0.988 was obtained. The adsorption capacity was high (437 mg/g) with an energy of adsorption (b) of 0.1. The dimensionless constant was low (0.042). This indicates that the adsorption of Cr(VI) onto ACLP was monolayer coverage of its surface.

The Freundlich isotherm constants for the plot of $\log q_e$ vs. $\log C_e$ are presented in Table 6. A high correlation coefficient (R^2) value of 0.981 was obtained. The plot was linear, which suggests that adsorption of Cr(VI) onto ACLP could be fairly described by the Freundlich isotherm model.

Several adsorbents have been investigated for Cr (VI) removal. However, the adsorption capacity of these adsorbents vary. Table 7 compares the adsorption capacity of ACLP with other adsorbents. It is significantly evident from Table 7 that ACLP has comparative advantage over other adsorbents.

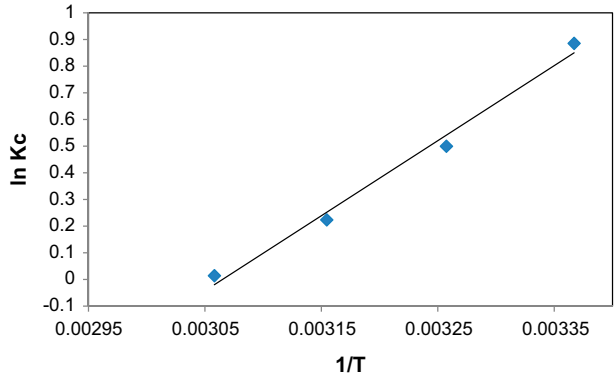

Fig. 6. Thermodynamics plot of ln K_c vs. $1/T$.

4.3. Thermodynamics study

The thermodynamic parameters obtained from the slope and intercept of the plot of ln K_c vs. $1/T$ (Fig. 6) are the enthalpy change (ΔH°) and entropy (ΔS°). The free energies were negative and decreased as temperature was increased. Negative free energies (ΔG°) indicate that adsorption was spontaneous for the temperature range evaluated and the degree of spontaneity increased as temperature was increased [44]. The negative value of the standard enthalpy change (ΔH° −23.41 kJ/mol) implies that the adsorption process was exothermic. The negative value of entropy change (ΔS° –71.8 J/mol) indicates increased randomness of the solution interface during adsorption of Cr (VI) onto ACLP. The thermodynamics constants are presented in Table 8.

5. Conclusion

Ageratum conyzoide leaf powder (ACLP) was utilized for the adsorption of Cr(VI) from aqueous solution. Experiments were designed with RSM and results showed that the removal efficiency exceeded 90% from initial concentration of 50 mg/L. The predicted model was successfully optimized by RSM. Solution pH was the most significant variable for Cr (VI) adsorption. Adsorption kinetics were best described by the pseudo-second-order kinetic model. Equilibrium study showed favorable description by Langmuir isotherm and fair representation by Freundlich isotherm. Thermodynamic parameters indicate

that adsorption of Cr(VI) onto ACLP was exothermic and physiosorption. ACLP being an abundant adsorbent could be put to beneficial use in the treatment of contaminated wastewater.

Acknowledgment

This study was supported by Universiti Teknologi Petronas (UTP) through its graduate scheme. The authors are therefore grateful to Universiti Teknologi Petronas.

References

[1] A.K. Shanker, C. Cervantes, H. Loza-Tavera, S. Avudainayagam, Chromium toxicity in plants, Environ. Int. 31 (2005) 739–753.
[2] K. Anupam, S. Dutta, C. Bhattacharjee, S. Datta, Adsorptive removal of chromium (VI) from aqueous solution over powdered activated carbon: Optimisation through response surface methodology, Chem. Eng. J. 173 (2011) 135–143.
[3] K. Muthukumaran, N. Balasubramanian, T.V. Ramakrishna, Removal and recovery of chromium from plating waste using chemically activated carbon, Met. Finish. 93 (1995) 46–53.
[4] World Health Organization, Environmental Health Criteria 61: Chromium, WHO, Geneva, Switzerland, 1988.
[5] H. Demiral, İ. Demiral, F. Tümsek, B. Karabacakoğlu, Adsorption of chromium(VI) from aqueous solution by activated carbon derived from olive bagasse and applicability of different adsorption models, Chem. Eng. J. 144 (2008) 188–196.
[6] K. Anupam, S. Dutta, C. Bhattacharjee, S. Datta, Artificial neural network modelling for removal of chromium (VI) from wastewater using physisorption onto powdered activated carbon, Desalin. Water Treat. 52 (2014) 1–10.
[7] A. Baran, E. Bıçak, Ş.H. Baysal, S. Önal, Comparative studies on the adsorption of Cr(VI) ions on to various sorbents, Bioresour. Technol. 98 (2007) 661–665.
[8] N.R. Bishnoi, M. Bajaj, N. Sharma, A. Gupta, Adsorption of Cr(VI) on activated rice husk carbon and activated alumina, Bioresour. Technol. 91 (2004) 305–307.
[9] M.N. Ahmed, R.N. Ram, Removal of basic dye from waste-water using silica as adsorbent, Environ. Pollut. 77 (1992) 79–86.
[10] M. Khalid, G. Joly, A. Renaud, P. Magnoux, Removal of phenol from water by adsorption using zeolites, Ind. Eng. Chem. Res. 43 (2004) 5275–5280.
[11] K.R. Srinivasan, H.S. Fogler, Use of inorgano-organoclays in the removal of priority pollutants from industrial wastewaters: Adsorption of benzo (a) pyrene and chlorophenols from aqueous solutions, Clays Clay Miner. 38 (1990) 287–293.
[12] S.P. Dubey, K. Gopal, Adsorption of chromium(VI) on low cost adsorbents derived from agricultural waste material: A comparative study, J. Hazard. Mater. 145 (2007) 465–470.
[13] V. Garg, R. Gupta, R. Kumar, R. Gupta, Adsorption of chromium from aqueous solution on treated sawdust, Bioresour. Technol. 92 (2004) 79–81.
[14] A. Bhattacharya, T. Naiya, S. Mandal, S. Das, Adsorption, kinetics and equilibrium studies on removal of Cr(VI) from aqueous solutions using different low-cost adsorbents, Chem. Eng. J. 137 (2008) 529–541.
[15] S.H. Hasan, D. Ranjan, M. Talat, Water hyacinth biomass (WHB) for the biosorption of hexavalent chromium: Optimization of process parameters, BioResources 5 (2010) 563–575.
[16] K.G. Bhattacharyya, A. Sharma, Kinetics and thermodynamics of Methylene Blue adsorption on Neem (*Azadirachta indica*) leaf powder, Dyes Pigm. 65 (2005) 51–59.
[17] V. Ponnusami, R. Aravindhan, N. Karthik Raj, G. Ramadoss, S. Srivastava, Adsorption of methylene blue onto gulmohar plant leaf powder: Equilibrium, kinetic, and thermodynamic analysis, J. Environ. Prot. Sci. 3 (2009) 1–10.
[18] V. Ponnusami, S. Vikram, S. Srivastava, Guava (*Psidium guajava*) leaf powder: Novel adsorbent for removal of methylene blue from aqueous solutions, J. Hazard. Mater. 152 (2008) 276–286.
[19] E.H. Ezechi, S.R.b.M. Kutty, A. Malakahmad, M.H. Isa, Characterization and optimization of effluent dye removal using a new low cost adsorbent: Equilibrium, kinetics and thermodynamic study, Process Saf. Environ. Prot. 98 (2015) 16–32.
[20] R.K. Kohli, D.R. Batish, H. Singh, K.S. Dogra, Status, invasiveness and environmental threats of three tropical American invasive weeds, Parthen. Hyster. 8 (2006) 1501–1510.
[21] R. Yadava, S. Kumar, A novel isoflavone from the stems of *Ageratum conyzoide*s, Fitoterapia 70 (1999) 475–477.
[22] J.H. Nogueira, E. Gonçalez, S.R. Galleti, R. Facanali, M.O. Marques, J.D. Felício, *Ageratum conyzoide*s essential oil as aflatoxin suppressor of *Aspergillus flavus*, Int. J. Food Microbiol. 137 (2010) 55–60.
[23] A. Moura, E. Silva, M. Fraga, A. Wanderley, P. Afiatpour, M. Maia, Antiinflammatory and chronic toxicity study of the leaves of *Ageratum conyzoides* L. in rats, Phytomedicine 12 (2005) 138–142.
[24] K. Anupam, S. Dutta, C. Bhattacharjee, S. Datta, Optimisation of adsorption efficiency for reactive red 198 removal from wastewater over TiO_2 using response surface methodology, Can. J. Chem. Eng. 89 (2011) 1274–1280.
[25] E.H. Ezechi, M.H. Isa, S.R. bin Mohamed Kutty Z. Ahmed, Electrochemical removal of boron from produced water and recovery, J. Environ. Chem. Eng. 3 (2015) 1962–1973.
[26] E.H. Ezechi, S.R.M.b. Kutty, A. Malakahmad, I.U. Salihi, N. Aminu, Determination of optimum range for hexavalent chromium Cr(VI) removal using *ageratum conyzoide* leaf powder (ACLP), AIP Conf. Proc. 1669 (2015) 020014.
[27] E.H. Ezechi, S.R.M.b. Kutty, A. Malakahmad, M.H. Isa, N. Aminu, I.U. Salihi, Removal of methylene blue from dye effluent using *ageratum conyzoide* leaf powder (ACLP), AIP Conference Proceedings 1669 (2015) 020013.

[28] M.H. Isa, E.H. Ezechi, Z. Ahmed, S.F. Magram, S.R.M. Kutty, Boron removal by electrocoagulation and recovery, Water Res. 51 (2014) 113–123.
[29] S. Peng, S. Wang, T.J.S. Chen, Thermodynamics study of adsorption of water soluble dyestuffs onto purified palygorskite, J. Chin. Ceram. Soc. 8 (2005) 1012–1017.
[30] S. Mohajeri, H.A. Aziz, M.H. Isa, M.A. Zahed, M.N. Adlan, Statistical optimization of process parameters for landfill leachate treatment using electro-Fenton technique, J. Hazard. Mater. 176 (2010) 749–758.
[31] M.J. Bashir, H.A. Aziz, M.S. Yusoff, M.N. Adlan, Application of response surface methodology (RSM) for optimization of ammoniacal nitrogen removal from semi-aerobic landfill leachate using ion exchange resin, Desalination 254 (2010) 154–161.
[32] K. Huang, Y. Xiu, H. Zhu, Selective removal of Cr(VI) from aqueous solution by adsorption on mangosteen peel, Environ. Sci. Pollut. Res. 20 (2013) 5930–5938.
[33] N.K. Hamadi, X.D. Chen, M.M. Farid, M.G. Lu, Adsorption kinetics for the removal of chromium(VI) from aqueous solution by adsorbents derived from used tyres and sawdust, Chem. Eng. J. 84 (2001) 95–105.
[34] M. Dakiky, M. Khamis, A. Manassra, M. Mer'eb, Selective adsorption of chromium(VI) in industrial wastewater using low-cost abundantly available adsorbents, Adv. Environ. Res. 6 (2002) 533–540.
[35] S. Deng, R. Bai, Removal of trivalent and hexavalent chromium with aminated polyacrylonitrile fibers: Performance and mechanisms, Water Res. 38 (2004) 2424–2432.
[36] D. Kratochvil, P. Pimentel, B. Volesky, Removal of trivalent and hexavalent chromium by seaweed biosorbent, Environ. Sci. Technol. 32 (1998) 2693–2698.
[37] H.K. Boparai, M. Joseph, D.M. O'Carroll, Kinetics and thermodynamics of cadmium ion removal by adsorption onto nano zerovalent iron particles, J. Hazard. Mater. 186 (2011) 458–465.
[38] E.H. Ezechi, M.H. Isa, S.R.M. Kutty, "Removal of Boron from produced water by electrocoagulation, in: 10th WSEAS International Conference on Environment, Ecosystems and Development (EED'12), Switzerland, (2012) 87–92.
[39] W. Weber, J. Morris, Kinetics of adsorption on carbon from solution, J. Sanit. Eng. Div. Am. Soc. Civ. Eng. 89 (1963) 31–60.
[40] D. Sparks, Kinetics of reactions in pure and in mixed systems, Soil Physical Chemistry, CRC Press, Boca Raton, FL, 1986 , pp. 83–145.
[41] S.S. Gupta, K.G. Bhattacharyya, Adsorption of Ni(II) on clays, J. Colloid Interface Sci. 295 (2006) 21–32.
[42] S. Vasudevan, J. Lakshmi, G. Sozhan, Electrochemically assisted coagulation for the removal of boron from water using zinc anode, Desalination 310 (2013) 122–129.
[43] E.H. Ezechi, M.H. Isa, S.R.M. Kutty, A. Yaqub, Boron removal from produced water using electrocoagulation, Process Saf. Environ. Protect. 92 (2014) 509–514.
[44] Q. Li, Q.Y. Yue, Y. Su, B.Y. Gao, H.J. Sun, Equilibrium, thermodynamics and process design to minimize adsorbent amount for the adsorption of acid dyes onto cationic polymer-loaded bentonite, Chem. Eng. J. 158 (2010) 489–497.